

IR spectroscopy of gas-phase C_{60}^-

Peter Kupser,^a Jeffrey D. Steill,^b Jos Oomens,^b Gerard Meijer^a and Gert von Helden^{*a}

Received 11th July 2008, Accepted 3rd September 2008

First published as an Advance Article on the web 9th October 2008

DOI: 10.1039/b811862k

We present the IR spectrum of the gas-phase C_{60}^- anion. The C_{60}^- anions are mass-selected and trapped in an ion cyclotron mass spectrometer cell. The spectrum is obtained by recording the yield of electrons following infrared multiple photon absorption and subsequent electron detachment of the anions. Two bands are observed that correlate to two of the four IR-allowed transitions in neutral C_{60} . The results show that the higher frequency band is strongly shifted from its position in neutral C_{60} and is a sensitive marker for the charge state. The band positions and intensities are compared to results obtained by theory as well as to known bands in solid samples and good agreement is found.

1. Introduction

Fullerenes and fullerene-based materials attract a lot of attention and are the focus of thousands of publications. The solid-state properties of doped fullerene materials are especially of interest. When bulk C_{60} is doped with alkali atoms, intercalated compounds M_nC_{60} ($n = 1, 3, 4$ or 6) can form.^{1–4} In those materials, the alkali atoms transfer charge to the fullerene, giving rise to C_{60}^{n-} ions surrounded by n alkali ions. It is observed that M_nC_{60} with $n = 4$ behaves as an insulator while, for example, with $n = 3$ metallic behavior can be found. Depending on the metal, some even have superconducting properties^{2–4} and recently, Cs_3C_{60} was synthesized showing a threshold to superconductivity of 38 K—so far the highest value for a molecular system.⁵

It thus comes as no surprise that the properties and the electronic structure of C_{60}^{n-} anions are of special interest. The addition of one or more electrons can cause Jahn–Teller (JT) distortion.⁶ For C_{60} and other fullerenes, this distortion has been investigated both theoretically^{6–9} and experimentally.^{10–15} Especially C_{60}^- serves as a model system for the JT effect in highly symmetrical molecules and the molecule is expected to experience a distortion from icosahedral (I_h) to either D_{5d} or D_{3d} symmetry.⁶ In the solid state, Rb_1C_{60} has been investigated using IR reflectivity measurements.¹⁶ These studies show that the position of the highest frequency IR-allowed mode of icosahedral C_{60} is sensitive to the charge state. However, questions have been raised as to the role of the counter ions, and, in order to minimize their interactions, special compounds have been synthesized and investigated.^{15,17,18}

C_{60}^- has also been studied in the gas phase. Using photoelectron spectroscopy, the electron affinity of neutral C_{60} is determined to be 2.70 eV.¹¹ C_{60}^{2-} can be observed in the gas phase as well.¹⁹ It is, however, only metastable and can decay

to C_{60}^- and a free electron.²⁰ C_{60}^- is also investigated spectroscopically in an ion storage ring. From these measurements, it is concluded that C_{60}^- is dynamically distorted to presumably D_{3d} symmetry.¹³

Previously, it was shown that neutral gas-phase C_{60} can be efficiently excited using tunable IR light from a free-electron laser.^{21–23} When the radiation is resonant with an IR-allowed transition in the molecule, the sequential absorption of hundreds of photons can take place, resulting in very hot molecules. These hot molecules can cool by the emission of an electron and the positively charged C_{60}^+ can be detected as a function of IR wavelength. Plotting the ion yield as a function of wavelength gives a spectrum which was shown to be similar (but not equal) to the linear absorption spectrum. Here we show that gas-phase C_{60}^- can be excited using IR light and that the hot molecules can detach an electron. The detachment yield can be monitored as a function of wavelength, yielding an IR spectrum of C_{60}^- .

2. Experimental

The experiments are performed at the FOM-Institute for Plasma Physics “Rijnhuizen” in the Netherlands using the free-electron laser for infrared experiments (FELIX).²⁴ C_{60} anions are generated *via* electrospray ionization (ESI) and transported to and accumulated in a hexapole ion trap. The ions are then transferred into a home-built Fourier transform ion cyclotron resonance (FT-ICR) mass spectrometer based on a 4.7 T superconducting magnet.²⁵ Trapping, mass-selective isolation, and detection of the ions, as well as irradiation with IR photons is done inside the ICR cell. A leak valve allows for the admission of reactant gases.

C_{60} was obtained from MER company, Texas, whereas all other chemicals were purchased from Sigma-Aldrich. C_{60} anions are generated using the ESI source in a procedure developed by Kappes and coworkers.²⁶ C_{60} is dissolved in 1,2-dichlorobenzene at a concentration of 500 μ M. As electron donor for the fullerenes, a solution of 10 mM (tetrakis)-dimethylaminoethylene (TDAE) in toluene is used. Due to

^a Fritz-Haber-Institut der Max-Planck-Gesellschaft, Faradayweg 4–6, 14195 Berlin, Germany. E-mail: helden@fhi-berlin.mpg.de

^b FOM Institute for Plasma Physics Rijnhuizen, Edisonbaan 14, NL-3439 MN Nieuwegein, The Netherlands

its sensitivity to oxygen, the TDAE solution is prepared under nitrogen atmosphere. In order to avoid blocking of the 125 μm diameter stainless steel ESI capillary with aggregates produced in the solution and to improve the signal stability, the two solutions are mixed just before injection into the capillary. For this purpose, each solution is supplied by its own syringe pump (Harvard Apparatus 11plus). The solutions are combined, passed through a 5 μm filter and enter the ESI capillary. The flow rates are set to 1 $\mu\text{l min}^{-1}$ for the TDAE solution and 2 $\mu\text{l min}^{-1}$ for the fullerene solution. The ESI needle voltage is adjusted to -3 kV and the cone voltage to around -60 V.

The anions are transferred to and trapped in the ICR cell, which is optically accessible *via* a KRS-5 window at the back end. To maximize the overlap of the IR beam from FELIX with the ion cloud, a multipass arrangement is created using the polished inside surfaces of the excite plates of the cylindrical ICR cell.²⁷

FELIX is tunable over the range from 40 to 2000 cm^{-1} , although here we investigate only the 400–1700 cm^{-1} range. The light output comes in macropulses of 5 μs duration containing 0.3–5 ps long micropulses at a repetition rate of 1 GHz. The bandwidth is adjustable and transform limited by the micropulse duration. In the current experiments, the bandwidth amounts to approximately 0.5% of the central wavelength and at these settings, the pulse energy in a macropulse is about 35 mJ at the experiment.

In the present experiment, the irradiation time is set to 7.2 s with a macropulse repetition rate of 5 Hz. When the IR light is resonant with an IR active mode of the ion, the absorption of many photons can occur,²⁸ which can lead to the detachment of an electron. Although these electrons remain trapped in the ICR cell, their cyclotron frequency is too high to be detected by the data acquisition system. Nonetheless, they can be detected indirectly by monitoring reaction products of the electrons with electron capture agents, admitted to the ICR cell.^{29,30} In the present experiments, two different electron capture agents are used: SF_6 , yielding SF_6^- as reaction product, and CCl_4 , which undergoes dissociative electron attachment with Cl^- as product. Adding the neutral reaction partners raises the base pressure in the apparatus from around 1×10^{-8} to 1.4×10^{-7} Torr. IR spectra can then be obtained by either monitoring the depletion of the parent ion or the appearance of a reaction product as a function of IR wavelength.

Density functional theory (DFT) is used to calculate theoretical IR spectra. The calculations are performed with Turbomole V5.10³¹ using the B3LYP functional and the def2-SVP^{32–34} basis set. To generate starting geometries, icosahedral C_{60} is compressed or elongated along a C_3 , C_5 or C_2 symmetry axis to result in structures of D_{3d} , D_{5d} or D_{2h} symmetry respectively. Geometries are optimized in their respective symmetries and vibrational frequencies and IR intensities are calculated using analytical second derivatives.

3. Results and discussion

Mass spectra of isolated and subsequently irradiated C_{60}^- are recorded at different wavelengths of FELIX. If the IR photons are in resonance with an IR transition in the molecule, several

hundreds of photons can be absorbed. In general, several cooling pathways are possible for the hot molecules. The excited molecules may undergo fragmentation, detach an electron or emit radiation. At the excitation levels expected under our conditions, the latter process occurs only on a very long time scale and is not expected to be important here. All other processes cause a depletion of the parent ion signal. If the molecules undergo dissociation, this would have been observed as the appearance of additional peaks in the mass spectrum, which is not the case.

As mentioned above, detached electrons can not be detected directly, however, they can be monitored by admitting, for example, SF_6 or CCl_4 to the ICR cell. In the experiments presented here, reaction products of detached electrons are observed for both gases. However, Cl^- as a reaction product has the advantage that it cannot absorb IR radiation and hence cannot introduce artefacts caused by IR-induced dissociation of the product ion.

The appearance of Cl^- ions accompanied by a decrease in the parent ion signal in the mass spectrum is an indicator for an IR transition in the fullerene anion. Fig. 1 shows the appearance of Cl^- as a function of IR frequency together with a theoretical stick spectrum for C_{60}^- . In the experimental spectrum, the intensity is corrected for drift in the parent ion signal during a scan. Several spectra have been recorded and are averaged. At least three spectra were taken in every wavelength region, except between 850 and 970 cm^{-1} , where only one scan is performed. The spectra clearly show two peaks at 570 and 1374 cm^{-1} . The full width at half maximum of these bands is 6 and 27 cm^{-1} , respectively. On both resonances, the appearance of chloride ions is accompanied by a depletion of the C_{60}^- parent ion signal. In order to avoid saturation effects, the FELIX fluence is adjusted such as to keep the amount of depletion below 50%. The accuracy of the wavelength position is estimated to be $\pm 0.25\%$.

IR spectra of neutral C_{60} in thin films³⁵ as well as for neutral C_{60} in the gas phase are known.³⁶ For C_{60} in icosahedral symmetry, only the four T_{1u} out of 46 symmetry unique modes are IR-active. In solid C_{60} , in addition weak resonances caused by anharmonic couplings and/or symmetry reduction due to the environment can be observed³⁷ and the fundamental transitions are found at 527, 576, 1183 and 1429 cm^{-1} .

The IR spectrum of neutral C_{60} in the gas phase has been measured *via* IR emission spectroscopy³⁶ and IR resonance-enhanced multiple-photon ionization (IR-REMPI) spectroscopy of hot (875 K) C_{60} . There, the four T_{1u} modes are found at 518, 557, 1145 and 1397 cm^{-1} . In addition a combination band is observed at 1525 cm^{-1} . The positions of these modes shift to lower energies with increasing temperature of the molecules. For example, the $T_{1u}(4)$ mode is red-shifted by about 40 cm^{-1} at a temperature of 1830 K, compared to its value at 875 K.²³

Negatively charged C_{60} has been investigated intensively in solid-state compounds such as M_nC_{60} with $\text{M} = \text{K}$ or Rb and n ranging from one to six. In these compounds, each alkali atom donates one electron to C_{60} . In particular, infrared transmission as well as infrared reflectivity studies were performed on these compounds.^{16,38,39} In solid RbC_{60} four modes are found at 525 cm^{-1} ($T_{1u}(1)$), 574 cm^{-1} ($T_{1u}(2)$), 1182 cm^{-1}

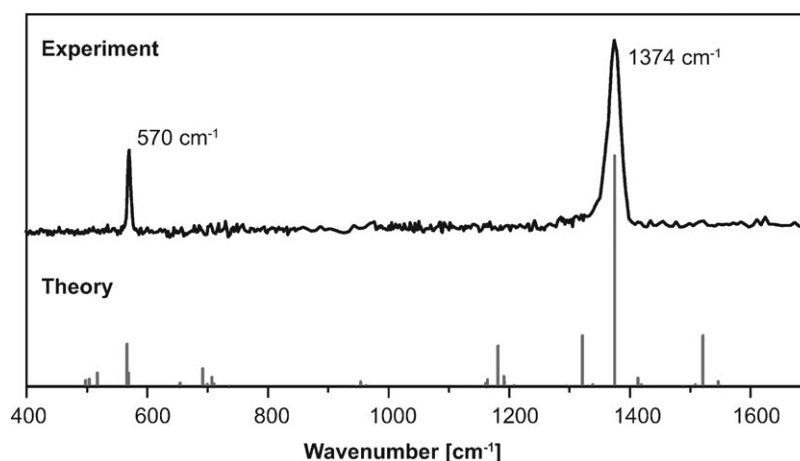


Fig. 1 Experimental IR spectrum of C_{60}^- , recorded *via* the measurement of the yield of Cl^- atoms as a function of IR frequency. The scaling of the ordinate is linear. No signal of chloride ions is obtained on the baseline. A theoretical spectrum for C_{60}^- in D_{3d} symmetry is shown as a stick spectrum. The calculations are performed using the B3LYP method and the def2-SVP basis set. Frequencies are scaled by 0.9648. See text for details.

($T_{1u}(3)$) and 1392 cm^{-1} ($T_{1u}(4)$).¹⁶ Compared to neutral C_{60} , the highest frequency $T_{1u}(4)$ band is observed to have the largest shift. The relative intensities also show a dramatic change with the $T_{1u}(1)$ and $T_{1u}(3)$ modes being very weak and barely observable.¹⁶ For M_nC_{60} , $n = 3$ and 4, the $T_{1u}(1)$ and $T_{1u}(3)$ modes are not observed at all. With increasing charge state, the $T_{1u}(4)$ band shows a pronounced shift to lower frequencies while the $T_{1u}(2)$ hardly shifts (see Table 1).

In M_nC_{60} , the C_{60} anion may be significantly perturbed by the alkali cations and this may have a significant effect on the electronic structure as well as on the position of the IR absorption bands. As a model system for the isolated C_{60} monoanion in a crystalline environment, C_{60} -tetraphenylphosphonium- and arsonium halides have been investigated. The fullerenes in these compounds are well separated from each other and surrounded by PhX^+ ($Ph = \text{phenyl} = C_6H_5$, $X = P$ or As as counterions).¹⁵ In their IR spectra, two resonances at positions similar to those for RbC_{60} are observed, with the low frequency mode showing a splitting of about 4 cm^{-1} (see Table 1).

Adding a single electron to neutral C_{60} is expected to cause Jahn–Teller distortion of the molecule. This lowers its symmetry from icosahedral to D_{3d} , D_{5d} or D_{2h} ,⁶ and experimental¹² as well as theoretical⁹ evidence indicates that the ground state is of D_{3d} symmetry. As a result of this symmetry

lowering, more transitions in the molecule are IR-allowed, potentially leading to additional bands in the spectrum. In order to assign the experimental spectrum, density functional calculations were performed using the B3LYP methods with the def2-SVP basis set. For C_{60}^- in D_{3d} , D_{5d} and D_{2h} symmetry, the geometries are optimized and the vibrational spectra calculated. The D_{3d} structure is found to be the lowest energy structure. Vibrational analysis reveals that this structure corresponds to a real minimum while the D_{5d} and D_{2h} structures are saddle points on the potential-energy surface, indicated by the presence of imaginary frequencies in their vibrational spectra. The D_{3d} structure is found to have a slightly oblate structure which is 2.38 eV below the optimized structure of neutral C_{60} in I_h symmetry. The position (scaled by 0.9648⁴⁰) and intensities of the calculated resonances are shown in Fig. 1. Comparing experiment and theory (see Table 1) shows that two strong transitions predicted by theory are observed in the experiment. The calculated low frequency band near 566 cm^{-1} actually consists of a mode of E_u symmetry and a weaker mode of A_{2u} symmetry shifted about 2 cm^{-1} to the blue. This splitting is small compared to the 6 cm^{-1} width of the measured band and is therefore not expected to be observable in our experiment. The calculated band at 1374.6 cm^{-1} is of E_u symmetry and stands alone. When comparing the experimental and theoretical peak

Table 1 Positions of the $T_{1u}(2)$ and $T_{1u}(4)$ vibrational bands of neutral and negatively charged C_{60} molecules. Shown are band positions obtained by IR transmission, reflectivity and absorption spectra on solid samples and IR-REMPI, as well as emission spectra for gas phase molecules. Also shown are results from density functional calculations. All values are given in cm^{-1}

Experiment (gas phase)	$T_{1u}(2)$	$T_{1u}(4)$	Experiment (solid state)	$T_{1u}(2)$	$T_{1u}(4)$
$C_{60}@875\text{ K}$ (IR-REMPI) ^a	557	1397	C_{60} (absorption) ^b	576	1429
C_{60} (emission) ^c	570	1411			
$C_{60}(I_h)$ (theory) ^d	569	1418			
C_{60}^- (e^- detach.) ^e	570	1374	$(Ph_4As)_2ClC_{60}^f$	575 & 579	1387
C_{60}^- (D_{3d}) (theory) ^d	566	1375	Rb_1C_{60} (refl.) ^g	574	1392
			K_3C_{60} (refl.) ^g	572	1363
			Rb_3/K_3C_{60} (transm.) ^h	573	1393

^a Ref. 23. ^b Ref. 37. ^c Ref. 36. ^d Calculations scaled by 0.9648. ^e Presented in this work. ^f Ref. 15. ^g Ref. 16. ^h Ref. 39.

positions, one can notice that theory fits experiment very well and that the deviation is only about 0.7% (see Table 1).

In the experiment, two bands are observed while theory predicts the presence of additional IR-allowed modes in this frequency range. This discrepancy is possibly due to the excitation mechanism. C_{60} has an electron affinity of 2.70 eV.¹¹ However, for a thermal detachment of the electron to occur on our experimental timescale, the internal energy needs to be several times higher. Thus, at around 500 cm^{-1} , more than 100 photons need to be absorbed for electron detachment to take place. The experimental spectrum is therefore not to be considered as a linear absorption spectrum. IR radiation from FELIX has previously been used to resonantly excite neutral C_{60} followed by thermal ionization.²¹ For that process to occur, several hundreds of photons need to be absorbed by a single molecule. The resulting IR-REMPI spectrum shows the presence of all four IR-allowed modes, plus one combination band. It is observed, however, that the measured relative intensities do not correspond to the calculated ones. Those observations could be explained by the excitation mechanism and the anharmonicities of the vibrational modes.^{22,23} The absorption of a single IR photon is followed by fast intramolecular vibrational redistribution (IVR), depositing the energy in the bath of vibrational states and thereby effectively de-exciting the absorbing mode. This process can occur many times during a FELIX macropulse. During that process, the internal energy rises, causing anharmonicities to induce a red-shift of the absorbing mode. When the anharmonicity is large, the red-shift can limit the number of absorbed photons, as the mode shifts out of the bandwidth of the IR radiation. A very similar excitation mechanism is applicable here as well. The relative intensities in the experimental spectrum are influenced and it is possible that the modes that are not observed have a low oscillator strength and/or a large anharmonicity. Another related effect is important too. For the low frequency mode, theory predicts two closely spaced bands. During the excitation process, while the lower frequency mode shifts out of the laser bandwidth, the mode to the blue side can shift into resonance.²⁸ Thus, while theory predicts the $T_{1u}(2)$ mode to be not much more intense than some of the modes that are not observed, the weaker mode to the blue can result in an enhancement of the excitation efficiency. In addition, in the IR-REMPI experiment, FELIX was tightly focused leading to a very high IR intensity. In the present experiment, due to constraints imposed by the experimental setup, FELIX is not focused as tightly, resulting in an at least one order of magnitude lower fluence. We expect that, with a higher fluence, more bands will be observable.

The anharmonicities, together with the spectral profile of the IR laser, determine not only the excitation efficiencies but also influence the peak positions and shapes in the spectrum. Modeling shows that peaks can have an asymmetry and a tail on their red side.^{22,23} In agreement with that, one can notice that the most intense peak at 1374 cm^{-1} is slightly asymmetric. More important here is the possibility of peak shifts. However, it is not likely that this effect is dramatic, as this shift is expected to be less than the spectral width of the excitation laser, which is 0.5–1 % FWHM of the center frequency in the present experiment.

For C_{60} anions in the solid, it is observed that the vibrational modes shift to the red with increasing negative charge (see Table 1; references are given there). This shift is small for the $T_{1u}(2)$ mode around 570 cm^{-1} , but large for the $T_{1u}(4)$ mode, which shifts from 1392 cm^{-1} for Rb_1C_{60} to 1340 cm^{-1} for Rb_6C_{60} . The value of 1374 cm^{-1} reported here for the $T_{1u}(4)$ mode is slightly lower than the values reported for C_{60} with nominally one negative charge. In experiments on solid state materials, the charge transfer to C_{60} might be incomplete and moreover, C_{60} anions might be significantly perturbed by the surrounding cations. In the present experiments, the charge on C_{60} is -1 and the ions are not perturbed by any surroundings. In agreement with that, the here presented value for the $T_{1u}(4)$ of C_{60}^- is closest to the value reported for solid-state materials which are designed to limit the interactions of C_{60} anions with the surroundings.¹⁵

4. Conclusions

The infrared spectrum of isolated room temperature C_{60}^- is presented. Two vibrational modes are found at 570 and 1374 cm^{-1} . The bands correlate to two of the four IR-allowed transitions in neutral C_{60} . The results show that the higher frequency band is strongly shifted from its position in neutral C_{60} and is a sensitive marker for the charge state. The measured spectrum is in good agreement with calculated spectra for Jahn–Teller distorted C_{60}^- with D_{3d} symmetry. The band positions and intensities are compared to results obtained by theory as well as to known bands in solid samples and good agreement is found.

Acknowledgements

We want to thank Dr Robert C. Dunbar for helpful discussions. We gratefully acknowledge the support by the Stichting voor Fundamenteel Onderzoek der Materie (FOM) in providing the required beam time on FELIX and highly appreciate the skillful assistance by the FELIX staff, in particular Dr B. Redlich and Dr A. F. G. van der Meer.

References

- 1 R. C. Haddon, A. F. Hebard, M. J. Rosseinsky, D. W. Murphy, S. J. Duclos, K. B. Lyons, B. Miller, J. M. Rosamilia, R. M. Fleming, A. R. Kortan, S. H. Glarum, A. V. Makhija, A. J. Muller, R. H. Eick, S. M. Zahurak, R. Tycko, G. Dabbagh and F. Thiel, *Nature*, 1991, **350**(6316), 320–322.
- 2 A. F. Hebard, M. J. Rosseinsky, R. C. Haddon, D. W. Murphy, S. H. Glarum, T. T. M. Palstra, A. P. Ramirez and A. R. Kortan, *Nature*, 1991, **350**(6319), 600–601.
- 3 K. Holczer, O. Klein, S. M. Huang, R. B. Kaner, K. J. Fu, R. L. Whetten and F. Diederich, *Science*, 1991, **252**(5009), 1154–1157.
- 4 M. J. Rosseinsky, A. P. Ramirez, S. H. Glarum, D. W. Murphy, R. C. Haddon, A. F. Hebard, T. T. M. Palstra, A. R. Kortan, S. M. Zahurak and A. V. Makhija, *Phys. Rev. Lett.*, 1991, **66**(21), 2830–2832.
- 5 A. Y. Ganin, Y. Takabayashi, Y. Z. Khimyak, S. Margadonna, A. Tamai, M. J. Rosseinsky and K. Prassides, *Nature*, 2008, **7**, 367–371.
- 6 C. C. Chancey and M. C. M. O'Brien, *The Jahn–Teller Effect in C_{60} and Other Icosahedral Complexes*, Princeton University Press, Princeton, NJ, 1997.
- 7 F. Negri, G. Orlandi and F. Zerbetto, *Chem. Phys. Lett.*, 1988, **144**(1), 31–37.

- 8 N. Koga and K. Morokuma, *Chem. Phys. Lett.*, 1992, **196**, 191–196.
- 9 W. H. Green, S. M. Gorun, G. Fitzgerald, P. W. Fowler, A. Ceulemans and B. C. Titeca, *J. Phys. Chem.*, 1996, **100**(36), 14892–14898.
- 10 D. R. Lawson, D. L. Feldheim, C. A. Foss, P. K. Dorhout, C. M. Elliott, C. R. Martin and B. Parkinson, *J. Electrochem. Soc.*, 1992, **139**(7), L68–L71.
- 11 O. Gunnarsson, H. Handschuh, P. S. Bechthold, B. Kessler, G. Gantefor and W. Eberhardt, *Phys. Rev. Lett.*, 1995, **74**(10), 1875–1878.
- 12 V. C. Long, J. L. Musfeldt, K. Kamáras, A. Schilder and W. Schütz, *Phys. Rev. B*, 1998, **58**(21), 14338–14348.
- 13 S. Tomita, J. U. Andersen, E. Bonderup, P. Hvelplund, B. Liu, S. Brøndsted Nielsen, U. V. Pedersen, J. Rangama, K. Hansen and O. Echt, *Phys. Rev. Lett.*, 2005, **94**(5), 53002.
- 14 G. Klupp, K. Kamáras, N. M. Nemes, C. M. Brown and J. Leão, *Phys. Rev. B*, 2006, **73**(8), 085415.
- 15 V. C. Long, E. C. Schundler, G. B. Adams, J. B. Page, W. Bietsch and I. Bauer, *Phys. Rev. B*, 2007, **75**(12), 125402.
- 16 T. Pichler, R. Winkler and H. Kuzmany, *Phys. Rev. B*, 1994, **49**(22), 15879–15889.
- 17 P.-M. Allemand, G. Srdanov, A. Koch, K. Khemani, F. Wudl, Y. Rubin, F. Diederich, M. M. Alvarez, S. Anz and R. L. Whetten, *J. Am. Chem. Soc.*, 1991, **113**, 2780–2781.
- 18 A. Pénicaud, A. Pérez-Benítez, R. Gleason, V. E. Muñoz and P. R. Escudero, *J. Am. Chem. Soc.*, 1993, **115**(22), 10392–10393.
- 19 P. A. Limbach, L. Schweikhard, K. A. Cowen, M. T. McDermott, A. G. Marshall and J. V. Coe, *J. Am. Chem. Soc.*, 1991, **113**, 6795–6798.
- 20 O. Hampe, M. Neumaier, M. N. Blom and M. M. Kappes, *Chem. Phys. Lett.*, 2002, **354**, 303–309.
- 21 G. von Helden, I. Holleman, G. M. H. Knippels, A. F. G. van der Meer and G. Meijer, *Phys. Rev. Lett.*, 1997, **79**(26), 5234–5237.
- 22 G. von Helden, I. Holleman, G. Meijer and B. Sartakov, *Opt. Express*, 1999, **4**(2), 46–52.
- 23 A. Bekkerman, E. Kolodney, G. von Helden, B. Sartakov, D. van Heijnsbergen and G. Meijer, *J. Chem. Phys.*, 2006, **124**(18), 184312.
- 24 D. Oepts, A. F. G. van der Meer and P. W. van Amersfoort, *Infrared Phys. Technol.*, 1995, **36**(1), 297–308.
- 25 J. J. Valle, J. R. Eyler, J. Oomens, D. T. Moore, A. F. G. van der Meer, G. von Helden, G. Meijer, C. Hendrickson, A. G. Marshall and G. Blakney, *Rev. Sci. Instrum.*, 2005, **76**(2), 023103.
- 26 B. Concina, M. Neumaier, O. Hampe and M. M. Kappes, *Int. J. Mass Spectrom.*, 2006, **252**(2), 110–116.
- 27 N. C. Polfer and J. Oomens, *Phys. Chem. Chem. Phys.*, 2007, **9**(29), 3804–3817.
- 28 J. Oomens, B. G. Sartakov, G. Meijer and G. von Helden, *Int. J. Mass Spectrom.*, 2006, **254**(1–2), 1–19.
- 29 R. N. Rosenfeld, J. M. Jasinski and J. I. Brauman, *J. Chem. Phys.*, 1979, **71**(2), 1030–1031.
- 30 J. D. Steill and J. Oomens, *J. Phys. Chem. A*, submitted. arXiv: 0809.2519v1.
- 31 R. Ahlrichs, M. Bär, M. Häser, H. Horn and C. Kölmel, *Chem. Phys. Lett.*, 1989, **162**(3), 165–169.
- 32 O. Treutler and R. Ahlrichs, *J. Chem. Phys.*, 1995, **102**(1), 346–354.
- 33 K. Eichkorn, F. Weigend, O. Treutler and R. Ahlrichs, *Theor. Chem. Acc.*, 1997, **97**(1–4), 119–124.
- 34 A. Schäfer, H. Horn and R. Ahlrichs, *J. Chem. Phys.*, 1992, **97**(4), 2571–2577.
- 35 W. Krättschmer, K. Fostiropoulos and D. R. Huffman, *Chem. Phys. Lett.*, 1990, **170**(2–3), 167–170.
- 36 L. Nemes, R. S. Ram, P. F. Bernath, F. A. Tinker, M. C. Zumwalt, L. D. Lamb and D. R. Huffman, *Chem. Phys. Lett.*, 1994, **218**(4), 295–303.
- 37 K. A. Wang, A. M. Rao, P. C. Eklund, M. S. Dresselhaus and G. Dresselhaus, *Phys. Rev. B*, 1993, **48**(15), 11375–11380.
- 38 T. Pichler, M. Matus and H. Kuzmany, *Solid State Commun.*, 1993, **86**(4), 221–225.
- 39 M. C. Martin, D. Koller and L. Mihaly, *Phys. Rev. B*, 1993, **47**(21), 14607–14610.
- 40 J. P. Merrick, D. Moran and L. Radom, *J. Phys. Chem. A*, 2007, **111**(45), 11683–11700.